Rock and Soil Mechanics

Volume 44 | Issue 5 Article 2

8-21-2023

Creep–fatigue constitutive model of salt rock based on a hardening parameter

Jin-yang FAN
State Key Laboratory for the Coal Mine Disaster Dynamics and Controls, Chongqing University, Chongqing 400044 China, School of Resources and Safety, Chongqing University, Chongqing 400044 China

Lu-xuan TANG
State Key Laboratory for the Coal Mine Disaster Dynamics and Controls, Chongqing University, Chongqing 400044 China, School of Resources and Safety, Chongqing University, Chongqing 400044 China

Jie CHEN
State Key Laboratory for the Coal Mine Disaster Dynamics and Controls, Chongqing University, Chongqing 400044 China, School of Resources and Safety, Chongqing University, Chongqing 400044 China

Zhen-yu YANG
State Key Laboratory for the Coal Mine Disaster Dynamics and Controls, Chongqing University, Chongqing 400044 China, School of Resources and Safety, Chongqing University, Chongqing 400044 China

See next page for additional authors

Creep–fatigue constitutive model of salt rock based on a hardening parameter

Authors
Jin-yang FAN, Lu-xuan TANG, Jie CHEN, Zhen-yu YANG, and De-yi JIANG

Rock and Soil Mechanics 2023 44(5): 1271−1282 ISSN 1000−7598
https: //doi.org/10.16285/j.rsm.2022.5877 http://rocksoilmech.researchcommons.org/journal

Creep–fatigue constitutive model of salt rock based on a hardening parameter

FAN Jin-yang[1, 2], TANG Lu-xuan[1, 2], CHEN Jie[1, 2], YANG Zhen-yu[1, 2], JIANG De-yi[1, 2]

1. State Key Laboratory for the Coal Mine Disaster Dynamics and Controls, Chongqing University, Chongqing 400044 China

2. School of Resources and Safety, Chongqing University, Chongqing 400044 China

Abstract: Salt rock has been recognized as an ideal medium for energy storage or oil and gas storage because of its good creep and self-healing characteristics. Accurate characterization and prediction of the complex mechanical behavior of salt rock is the basis for ensuring the safety of underground space utilization project of salt caverns. Based on proposed parameters of hardening and other characteristic factors, in this study, a new creep–fatigue constitutive model is developed for salt rock considering complex loading and unloading paths. Based on the dislocation mechanism of salt rock deformation, hyperbolic damping elements are introduced as state variables to characterize the degree of rock hardening. The influence of loading and unloading history on the deformation behavior of salt rock is considered according to the evolution of hardening parameters. Based on the stress–strain relation of the classical Norton model, a basic mathematical relation is established for the creep–fatigue constitutive model. By assuming the initial nucleation length and considering the material fracture toughness, the stress–strain relation is modified for the range of adjacent failure stage (accelerated deformation stage) based on a new introduced crack growth factor. In this manner, the proposed model can well predict the plastic deformation characteristics under complex loading and unloading paths, such as conventional creep, cyclic loading and unloading, lower-limit interval cyclic loading and unloading, and trapezoidal wave creep cyclic loading and unloading. The model can also better characterize the interaction between constant load creep and cyclic loading and unloading. Most of the model parameters have clear physical meanings in the new developed creep–fatigue constitutive model. Parameter *a* represents the relation factor between stress and deformation rate at the steady deformation stage of salt rock, parameter *b* determines the relation factor at the decelerated deformation stage of salt rock, and parameters d_0 and μ_d represent the initial crack nucleation amount and crack growth rate factor, respectively. The d_0 and μ_d jointly affect/modify the stress–strain relation at the critical failure stage of the model.

Keywords: salt rock; fatigue; creep; constitutive model

1 Introduction

Salt rock stratum has been recognized as an ideal place for oil and gas storage, compressed air energy storage, chemical liquid battery and CO_2 storage, and solid waste disposal due to its dense structure, low permeability and porosity, and good self-recovery property. The stress state and environment of surrounding rocks of salt cavern are complex under different engineering conditions. Because the natural gas storage in the salt cavern is affected by seasonal gas injection and extraction, the surrounding rocks are typical in a slow cyclic loading state. The surrounding rocks also suffer from rapid and high-frequency fatigue loading due to rapid and high-frequency air pressure fluctuations. Moreover, the salt rocks are subjected to high-temperature creep action for a long term because of radioactive heat from low-level radioactive nuclear waste. Therefore, many scholars[1−11] have conducted a large number of studies on the fatigue and creep deformation behavior of salt rocks based on the practical engineering requirements.

For understanding the creep characteristics of salt rocks with impurities, Wu et al.[12] performed triaxial creep tests on the salt rocks with two types of impurities under stepwise loading using a large program-controlled rheometer. They found that the confining pressure and impurity content affect the failure morphology and mechanical parameters of salt rocks and the creep capacity of low-impurity salt rocks is even stronger. Liang et al.[13] explored creep characteristics of glauberite salt rocks during in situ leaching mining, and performed triaxial creep tests on salt rocks under different osmotic pressures (3, 2 and 1 MPa). Liu et al.[14] conducted a laboratory uniaxial creep test on bedded salt rocks and monitored the acoustic emission signals during the test in real-time for 359 d. Xue et al.[15] performed a direct shear test on Pakistani salt rocks with high purity using direct shear test device YZW100, and analyzed the shear strength, shear deformation and damage mode of the salt rocks. They concluded that the cohesion and internal friction angle of Pakistani salt rocks are 7.41 MPa and 44.1°, respectively. Based on the triaxial fatigue–unloading tests of the marble specimens, Hou et al.[16] found that the rock strain is strongly sensitive to the decrease of confining pressure. Zhang et al.[17] investigated fatigue behavior and microstructural changes of salt rocks under cyclic loading, and the test results showed that the internal cracks of salt rocks were dominated by the generation of intergranular cracks under cyclic loading. They also concluded that the crack number increased

Received: 9 June 2022 Accepted: 13 September 2022
This work was supported by the National Natural Science Foundation project (52274073, 51834003), the Youth Program of National Natural Science Foundation (51904039) and the Graduate Research and Innovation Foundation of Chongqing, China (CYB20023).
First author: FAN Jin-yang, male, born in 1989, PhD, Professor, research interests: rock and soil mechanics, mining engineering, safety engineering. E-mail: Jinyang.f@cqu.edu.cn
Corresponding author: TANG Lu-xuan, female, born in 2000, Master degree, majoring in underground space stability. E-mail: 2812625915@qq.com

as the upper-limit stress ratio (i.e. the ratio of upper-limit stress to uniaxial compressive strength) increased.

It should be mentioned that the loading pattern of surrounding rocks shows large difference between the actual engineering project and the single cyclic loading and unloading or creeping tests in the laboratory. In addition to the typical cyclic loading, for instance, the compressed air energy storage of salt rocks is in an equilibrium state for a long time, i.e. no injection and no mining, and the pressure remains unchanged in a certain state. To this end, some coupled creep–fatigue tests have been conducted to study the interaction between the injection and production effects.

The creep–fatigue interaction is one of the typical behaviors of surrounding rocks of salt cavern. Wang et al.[18] found that the salt cavern reservoir project is affected by the combined influence of the occurrence environment and external disturbance. They found that the creep response of salt cavern is produced under the deviatoric stress, and the cumulative fatigue effect is also observed under cyclic loading and unloading conditions. Roberts et al.[19] conducted trapezoidal cyclic loading and unloading tests on salt mound-type salt rocks in the United States and studied the creep–fatigue deformation behavior of salt rocks under composite loading. To study the discontinuous fatigue evolution process of gas storage in the salt cavern under the action of intermittent periodic injection–production cycle, Li et al.[20] conducted triaxial interval fatigue tests by maintaining a minimum stress level for a period of time at the lower limit of cyclic loading. They found that the plastic deformation and damage evolution are accelerated by the interval effect during the fatigue process of salt rocks. Based on the discontinuous loading characteristics of compressed air energy storage in the salt cavern, Zhao et al.[21] studied the process of creep–fatigue induced damage evolution by maintaining a constant load for a certain period of time at the maximum stress level of cyclic loading. Ma et al.[22] conducted the same upper-limit interval cyclic loading and unloading tests, and found that the fatigue of salt rocks can be accelerated due to the cyclic loading and unloading.

The above-mentioned studies have shown that the creep behavior of salt rocks can affect the process of fatigue damage, and the cyclic loading and unloading can also change the creep rate. Although many fruitful studies have been conducted, most tests were performed in the laboratory. Moreover, a theoretical model that can describe the deformation behavior of salt rocks has not been established yet. A constitutive model considering the interaction between fatigue and creep needs to be built to increase the prediction accuracy of the mechanical characteristics under complex mechanical behavior of salt rocks. In this study, a new state variable is defined as the hardening parameter to characterize the rock hardening extent. This hardening parameter represents the modulus of the unloading deformation of a standard rock, i.e. the process of gradually losing the elastic recovery capacity. By introducing the hardening parameter and considering the influence of unloading and loading history on the deformation behavior of salt rocks, a new creep–fatigue constitutive model is developed to achieve a more accurate prediction of the deformation behavior of salt rocks under complex stress paths.

2 Creep–fatigue constitutive model

2.1 Analysis of constitutive model

The stress is in a constantly changing state during the fatigue process compared with the creep process. In a conventional fatigue process, the stress–strain relations can be described by either an elasto-plastic or visco-plastic constitutive model considering the hardening parameters[23–27]. The fatigue deformation process of salt rocks, especially for the low-cycle fatigue test, has many similar behaviors when compared to the creep deformation process, such as phase characteristics[28–30]. Both the creep and fatigue processes have a clear stage characteristics of deformation, which can be roughly divided into three stages: the decelerated deformation stage, the steady deformation stage, and the accelerated deformation stage. Therefore, a visco-plastic constitutive model is used to describe both creep and cyclic loading and unloading processes of salt rocks.

The existing creep models, such as Norton model and nonlinear creep model, can better predict the stage characteristics of deformation and is described by[31–35]

$$\dot{\varepsilon} = A\sigma^n \tag{1}$$

where $\dot{\varepsilon}$ is the deformation rate that is the first derivative of strain to time; σ is the stress; and A and n are the material factors. However, most of the constitutive models still have some limitations:

(1) The existing models are applicable to the 1st and 2nd deformation stages, i.e. the decelerated deformation stage and the steady deformation stage. The prediction error of the whole stage is relatively large, especially for the 3rd stage, i.e. the accelerated deformation stage before the critical failure.

(2) The existing models mainly consider the loading effect during the loading process, and the unloading process is not fully considered. This assumption leads to the same amount of visco-plastic deformation produced by the loading and unloading processes, which is not true in the laboratory test.

(3) The existing models do not consider the effect of historical unloading and loading stress paths on the visco-plastic behavior, i.e. the historical cumulative damage or cumulative hardening/softening behaviors is not considered.

2.2 New creep constitutive model

2.2.1 Hardening parameters (state variables)

Salt rock is a type of evaporitic sedimentary rock and mainly consists of NaCl polycrystals. The deformability of salt rock is associated with the internal dislocation density. The hardening degree inside the salt rock is related to the dislocation density, i.e. the larger the dislocation density, the greater the concentration of internal forces at the corresponding location. The state

variable σ^* is defined to characterize the hardening degree within the salt rock associated with the dislocation density. The state variable σ^* has the same magnitude and unit as the stress, and is calculated as

$$\frac{\sigma^*}{\sigma}=\frac{1}{1+c\sigma^m t^k} \tag{2}$$

$$\sigma^*=\frac{\sigma}{1+c\sigma^m t^k} \tag{3}$$

where c, m and k are the material factors; and t is the time.

As the stress is maintained constant, the state variable constantly approaches the value of stress σ. When the stress changes (only the loading process is considered herein), the equation is no longer applicable. The effect of the accumulated hardening degree needs to be taken into consideration. Assuming that the state variable is σ_0^* before the new stress is applied, and after a certain period of time, the new state variable can be expressed as

$$\left.\begin{aligned}\sigma^*&=\frac{\sigma}{1+c\sigma^m\left(t+\sigma_0^{-*}\right)^k}+\sigma_0^*\\ \sigma_0^{-*}&=\left(\frac{\sigma-\sigma_0^*}{c\sigma^m\sigma_0^*}\right)^{1/k}\end{aligned}\right\} \tag{4}$$

where σ_0^{-*} is the initial state variable.

In summary, the hardening parameter is a state variable characterized by stress and time. By changing the state variable value, the effect of creep–fatigue interaction on the deformation of salt rocks is achieved by continuous accumulation of deformation. Based on the variation of state variable, the constitutive model can then consider the effects of loading and unloading paths and time on deformation.

2.2.2 Stress–strain relation

The plastic deformation process of crystals is closely related to dislocation slip, proliferation and annihilation. At the first stage, large amount of the dislocation proliferation and slip occur. At the second stage, a dynamic balance state is reached between the dislocation proliferation and dislocation annihilation. Both the 1st and 2nd stages are strongly associated with dislocation proliferation[36–37]. Based on the relation between the steady creep rate and stress in the Norton model[31–35], the strain rate $\dot{\varepsilon}$ during the steady deformation stage is

$$\dot{\varepsilon}=a\sigma^n \tag{5}$$

where a is the material factor.

The deformation at the first stage mainly results from the dislocations that generated quickly and in a large quantity, i.e. influenced by the hardening parameter. The strain at this time is written as

$$\varepsilon=b\frac{\sigma^*}{\sigma}\sigma^n \tag{6}$$

where b is the material factor.

Combining Eqs. (5) and (6), the relation between stress and strain follows:

$$\varepsilon=\sigma^n\left(at+\frac{b}{1+c\sigma^m t^k}\right) \tag{7}$$

Equation (7) can also be re-written as

$$\varepsilon=\sigma^n\left(at+\frac{\sigma^*}{\sigma}b\right) \tag{8}$$

The first derivative of time for Eq. (8) is derived, and then the relation between the strain rate, stress and state variable is

$$\frac{\partial\varepsilon}{\partial t}=\dot{\varepsilon}=\sigma^n\left\{a-\frac{bck\sigma^m\left(t+\sigma_0^{-*}\right)^{k-1}}{\left[1+c\sigma^m\left(t+\sigma_0^{-*}\right)^k\right]^2}\right\} \tag{9}$$

From Eq. (9), one can see that the strain rate varies as the stress changes. In the loading state, as the stress loading rate is *v*, the state variable can be obtained by the integral of the following equation:

$$\sigma^*=ck\int\frac{\left(\sigma_0+vt\right)^{m+1}\left(t+\sigma_0^{-*}\right)^{k-1}}{\left[1+c\left(\sigma_0+vt\right)^m\left(t+\sigma_0^{-*}\right)^k\right]^2}\mathrm{d}t+\sigma_0^* \tag{10}$$

where σ_0 is the initial stress.

The strain during loading can be obtained from the following equation:

$$\begin{aligned}\varepsilon=&\int\left(\sigma_0+vt\right)^n\cdot\\ &\left\{a-\frac{bck\left(\sigma_0+vt\right)^m\left(t+\sigma_0^{-*}\right)^{k-1}}{\left[1+c\left(\sigma_0+vt\right)^m\left(t+\sigma_0^{-*}\right)^k\right]^2}\right\}\mathrm{d}t+\varepsilon_0=\\ &\int\left(\sigma_0+vt\right)^n\left(a+\frac{b\dot{\sigma}^*}{\sigma_0+vt}\right)\mathrm{d}t+\varepsilon_0\end{aligned} \tag{11}$$

where ε_0 is the initial strain.

2.2.3 Stress–strain relation during unloading process

When the rock material is in the unloading state, the external force may be less than the state variable. At this moment, the material is in the ‘over-hardening’ state, the reverse movement of dislocation occurs, and the local dislocation density decreases gradually. The state variable is written as

$$\sigma^*=\frac{\sigma}{1-c\sigma^m\left(t+\sigma_0^{-*}\right)^k} \tag{12}$$

The internal structure adjustment is completely dependent on the internal forces during unloading stage, and the adjustment rate is slow. A variable-speed creep unloading factor U_1 (state variable unloading factor) is introduced. The first derivative of time is derived to obtain the new state rate, which follows

$$\left.\begin{aligned}\dot{\sigma}^*&=U_1\frac{ck\sigma^{m+1}\left(t+\sigma_0^{-*}\right)^{k-1}}{\left[1-c\sigma^m\left(t+\sigma_0^{-*}\right)^k\right]^2}\\ \sigma_0^{-*}&=\left(\frac{\sigma_0^*-\sigma}{c\sigma^m\sigma_0^*}\right)^{1/k}\end{aligned}\right\} \tag{13}$$

The deformation rate of steady creep would also be affected. By introducing a new steady creep unloading factor U_2, the strain ε is calculated as

$$\varepsilon = \int (\sigma_0 + vt)^n \cdot \left\{ aU_2 + \frac{U_1 bCk(\sigma_0 + vt)^m \left(t + \sigma_0^{-*}\right)^{k-1}}{\left[1 - C(\sigma_0 + vt)^m \left(t + \sigma_0^{-*}\right)^k\right]^2} \right\} \mathrm{d}t + \varepsilon_0 \quad (14)$$

2.2.4 Stress–strain relation of the 3rd stage

At the 3rd stage of creep, the main reason for the acceleration characteristics is the crack expansion, and a crack expansion factor μ_d is therefore introduced. Crack formation is mainly generated by the dislocation accumulation. When the stress field and external stress field produced by a large number of dislocations superimpose, the strength factor reaches the fracture toughness and the crack is generated (or called the crack nucleation). The relevant evolutionary process of the crack nucleation has not been observed directly from rock tests and is tentatively considered as an instantaneous process. The initial nucleation length is assumed to be d_0, which is formed instantaneously. The formation moment is related to the stress applied externally and the accumulated plastic deformation, i.e.

$$K_\mathrm{c} = \Gamma(\sigma, \varepsilon) \quad (15)$$

where K_c is the fracture toughness, which is the essential attribute of material. Once the crack nucleation is formed, the length change rate $\dot{d}$ is

$$\dot{d} = \mu_\mathrm{d} \dot{\varepsilon} \quad (16)$$

where μ_d is the crack expansion factor; and $\dot{\varepsilon}$ is the deformation development rate.

$$d = \mu_\mathrm{d} \int \sigma_\mathrm{eff}^n \left\{ a - \frac{bck\sigma_\mathrm{eff}^m \left(t + \sigma_0^{-*}\right)^{k-1}}{\left[1 + c\sigma_\mathrm{eff}^m \left(t + \sigma_0^{-*}\right)^k\right]^2} \right\} \mathrm{d}t + d_0 \quad (17)$$

where σ_eff is the effective stress, which can be obtained by

$$\sigma_\mathrm{eff}(1 - d) + d\lambda\sigma = \sigma \quad (18)$$

Equation (18) can be re-written as

$$\sigma_\mathrm{eff} = \frac{1 - d\lambda}{1 - d}\sigma \quad (19)$$

where λ is the dynamic friction coefficient of crack surface.

At the 3rd stage, the deformation of salt rocks can be calculated as

$$\varepsilon = \int \sigma_\mathrm{eff}^n \left\{ a - \frac{bck\sigma_\mathrm{eff}^m \left(t + \sigma_0^{-*}\right)^{k-1}}{\left[1 + c\sigma_\mathrm{eff}^m \left(t + \sigma_0^{-*}\right)^k\right]^2} \right\} \mathrm{d}t + \varepsilon_0 \quad (20)$$

3 Model verification

In this section, the applicability of the developed creep–fatigue constitutive model is verified based on the laboratory test data of the salt rock specimens under different loading and unloading paths. The high-purity salt rock sampled from Pakistan is used, with NaCl content of 98% or more, containing a small amount of Na_2SO_4 and other impurities. The temperature and humidity are maintained constant during the whole test. The loading and unloading methods have four categories: constant load creep test, conventional cyclic loading and unloading fatigue test, trapezoidal wave loading and unloading creep–fatigue test, and lower-limit interval cyclic loading and unloading fatigue test.

3.1 Creep deformation

In the creep test on salt rocks, the stress level is set as 48 kN and the loading rate is set as 1 kN/s. The stress path is shown in Fig. 1. The change of the state variable to stress ratio (σ^*/σ) is shown in Fig. 2. Figure 3 shows the comparison between the model fitting results and laboratory creep test data, and Table 1 gives the model parameters of the creep test.

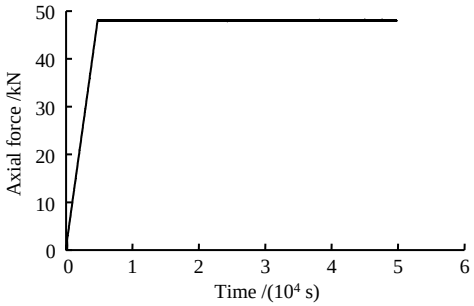

Fig. 1 Stress path of the creep test

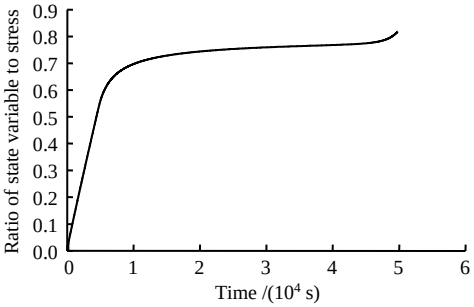

Fig. 2 Relation of state variable to stress ratio with time in the creep test

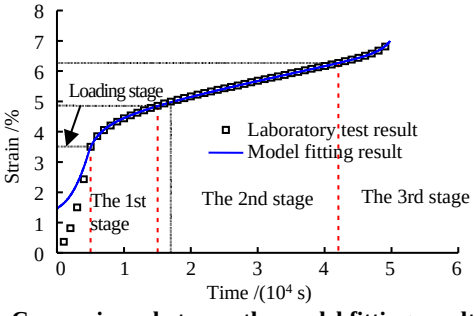

Fig. 3 Comparisons between the model fitting results and laboratory test data of the creep test

Table 1 Model parameters of the creep test

Stress /kN	*a*	*b*	*c*	*n*	*m*	*k*
48	7.36	7.3	100	2.3	0.92	–0.72

For the creep tests, it is found from Figs. 2 and 3 that the changes of state variable and stress are basically consistent with the variation trend of creep deformation. At the loading stage, as the axial force increases, the state variable to stress ratio increases linearly. After the stress is stable, the change of the state variable to stress ratio enters decelerated, steady and accelerated stages successively. It shows that the elastic deformation capacity of salt rocks is decreasing under a constant loading.

It can be roughly judged from Fig. 3 that the 2nd stage of creep starts at about 1.5×10^4 s, and the 3rd stage of creep starts at about 4.2×10^4 s. The loading of laboratory test starts from zero, and the condition of constant load creep test is not met at the loading stage, thus there is a large error in the fitting results. This means that the influence of loading path on the creep behavior needs to be considered in the data fitting analysis. When the stress reaches a constant state, the model prediction curve and the test data curve almost coincide with each other, and the overall fitting is good enough.

In summary, the developed model can well represent the three stages of the creep deformation of salt rocks. Considering the effects of time, load and state on creep characteristics, the state variable can better describe the deformation trend of salt rocks in creep test. Based on the fitting results, the proposed model can better reflect the three stages of salt rocks under loading condition, which indicates that the proposed model can better describe the creep characteristics of salt rocks with a good applicability.

3.2 Fatigue deformation

Cyclic loading and unloading fatigue tests are conducted for salt rock specimens. The upper stress level is set as 70 kN, the lower stress level is set as 3 kN, and the loading rate is set as 2 kN/s. The stress path is shown in Fig. 4. To show clearly, Fig. 4 only shows the first few stress cycles, and the same stress cycles are used for the test until the specimen is damaged. For the cyclic loading and unloading tests, the change of the state variable to stress ratio is shown in Fig. 5. The comparison between the model prediction results and the test data is shown in Fig. 6, and the model parameters are obtained as listed in Table 2. To show the fitting details, several comparison plots at different stages of fatigue deformation are given in Figs. 6(b)–6(d).

Based on Figs. 4 and 5, it is found that the state variable to stress ratio changes as the axial force varies. When the axial force increases, the ratio increases; when the axial force decreases, the ratio decreases. In the fatigue test on salt rocks, it is found from Figs. 5 and 6(a) that the change of state variable to stress ratio is basically consistent with the variation trend of fatigue deformation. Within a single cycle, the ratio

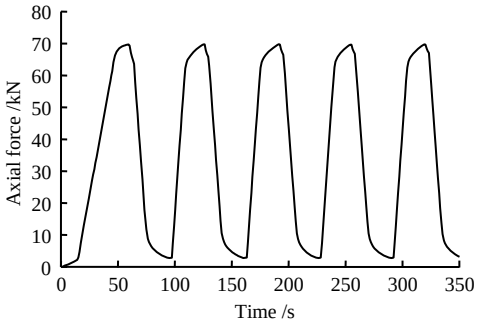

Fig. 4 Stress path of the fatigue test

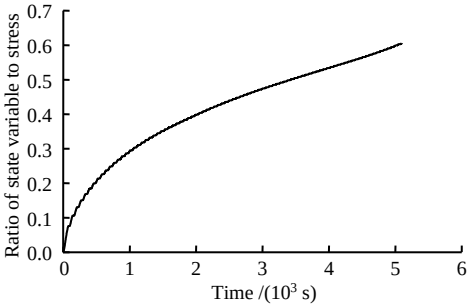

Fig. 5 Relation between state variable to stress ratio and time in the fatigue test

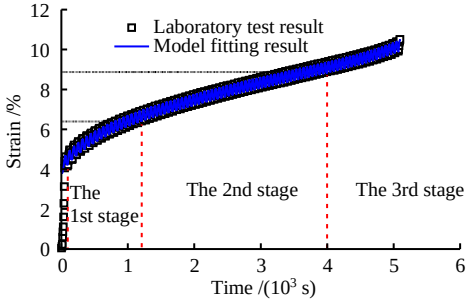

(a) Laboratory test result

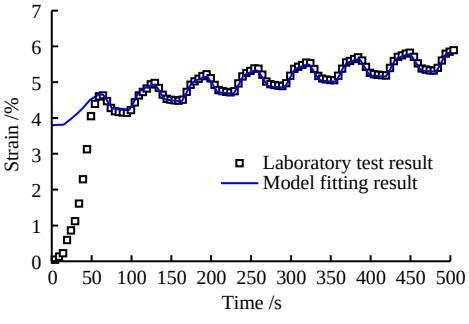

(b) The 1st stage

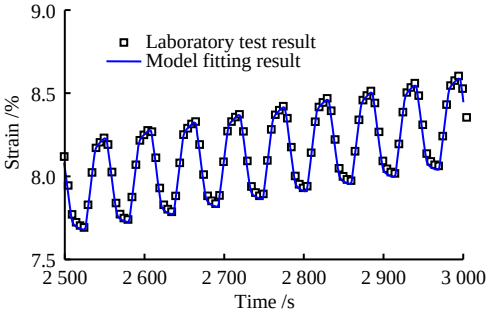

(c) The 2nd stage

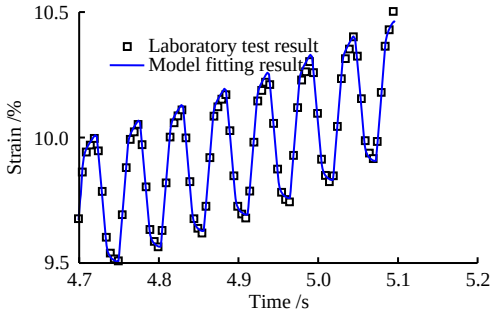

(d) The 3rd stage

Fig. 6 Comparisons between model fitting results and laboratory test data of the fatigue test

Table 2 Model parameters of the fatigue test

a	*b*	*c*	*n*	*m*	*k*
8	1.1	223	2.3	0.92	–0.72

varies more during loading and less during unloading, and the ratio changes greatly after the initial single cycle. As the cycle progresses, the variation of the single cycle ratio decreases continuously.

From Figs. 6(b)–6(d), it is shown that the proposed model can better predict the decelerated, steady and accelerated stages of fatigue deformation. There is a good fit between the test data and fitting results for the three stages. It should be mentioned that in Fig. 6(b), the fitting of the first cycle has a large error and the reason still lies in the first cycle loading stage.

Again, the developed model can well represent the three stages of the fatigue deformation of salt rocks. Considering the effects of time, load and state on the fatigue of salt rocks in the model, the state variable can better describe the deformation trend of salt rocks in the fatigue test. From the prediction/fitting results, it can be seen that the proposed model can well fit the three stages of salt rocks under loading conditions. It shows that the proposed model can well describe the fatigue deformation of salt rocks and has a good applicability.

3.3 Trapezoidal wave fatigue–creep deformation

A trapezoidal wave loading and unloading test is performed on the salt rock with a lower stress level of 2 kN, an upper stress level of 36 kN, a loading rate of 18 kN/h, and a cycle period of 7.6 h. The stress path is shown in Fig. 7. Unlike the fatigue test, the trapezoidal wave load is first loaded and maintained constantly, then unloaded and maintained constantly in one cycle, and each phase is maintained for 1.9 h. The change of state variables to stress ratio is shown in Fig. 8, and the test data are shown in Fig. 9(a) (the test is not conducted until the specimen is damaged due to the low stress level). The overall strain of salt rocks is divided into two stages: the decelerated stage and the steady stage. A comparison between the model fitting results and the test data for each stage is shown in Figs. 9(b) and 9(c), and the model parameters are listed in Table 3.

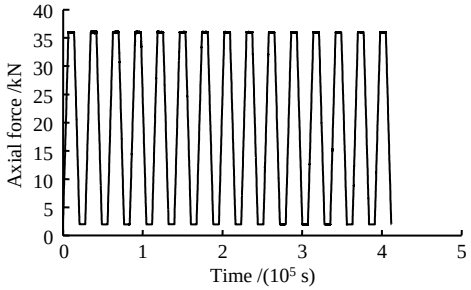

Fig. 7 Stress path of the trapezoidal wave test

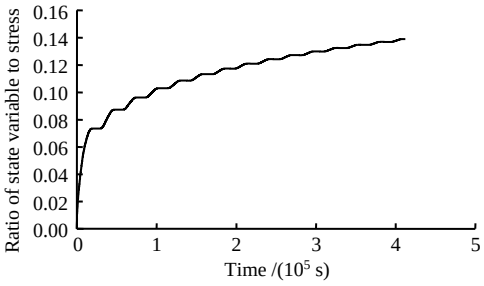

Fig. 8 Relation between state variable to stress ratio and time in the trapezoidal wave test

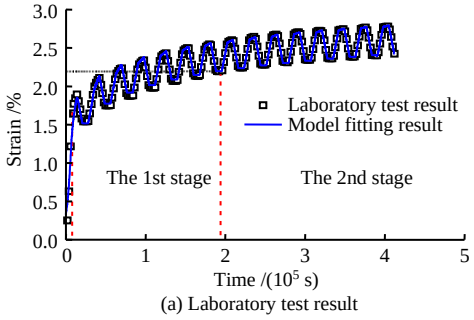

(a) Laboratory test result

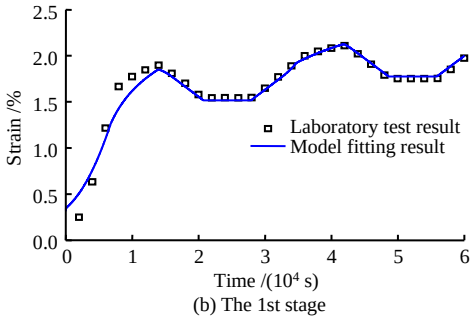

(b) The 1st stage

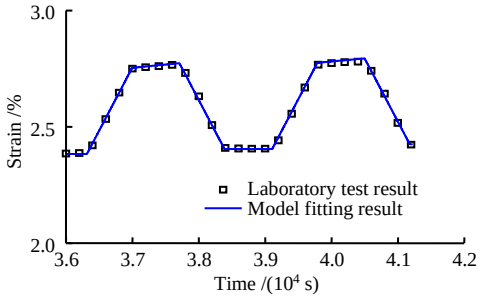

(c) The 2nd stage

Fig. 9 Comparisons between model fitting results and laboratory test data of the trapezoidal wave test

Table 3 Model parameters of the trapezoidal wave test

a	*b*	*c*	*n*	*m*	*k*
0.01	11	180	2.3	0.9	–0.55

In the trapezoidal wave loading and unloading test, it is observed from Figs. 8 and 9(a) that the change of state variable to stress ratio follows the same variation trend of the deformation for salt rocks. It also shows that the 1st stage changes greatly and as the time increases, the change of the ratio or strain decreases after a single cycle. The analysis in Fig. 8 shows that during loading in one cycle, the state variable to stress ratio increases, but remains almost constant during the constant loading or unloading stage. Under the combined effect of creep and fatigue, the result indicates that the deformation recovery capacity of salt rocks is damaged gradually during loading, while it is less affected during the constant loading or unloading condition.

From the comparison results between Figs. 9(b) and 9(c), the proposed model can better predict the interaction between fatigue and creep of salt rocks under trapezoidal wave loading. Similar to the creep and fatigue tests, there is a certain amount of error at the first cyclic loading stage. In addition, overall the strain has a consistent variation trend.

The proposed model can better describe the fatigue–creep deformation of salt rocks in the trapezoidal wave test. The variation of state variable to stress ratio can reflect the interaction between constant loading creep and cyclic loading and unloading fatigue during the deformation process. From the model prediction/ fitting results, it is observed that the proposed model can better fit the deformation of salt rocks under the interaction of creep and fatigue, and has a good applicability.

3.4 Lower-limit interval fatigue deformation

The fatigue deformation test under lower-limit interval cyclic loading and unloading is conducted on salt rocks. The upper stress level is set as 70 kN, the lower stress level is 2 kN, and the loading rate is 2 kN/s. After two cycles of loading and unloading, the time intervals are set as 5, 10, 15 and 20 min. Figure 10 shows the stress path for 5 min. To clearly show the details, only the first few specimens with stress cycles and intervals are selected. The same stress cycle and interval combinations are used in the test until the specimen is damaged. Based on the model fitting, the change between state variable to stress ratio is shown in Fig. 11, the comparison between the test data and the model fitting results is shown in Fig. 12, and the model parameters are obtained as listed in Table 4.

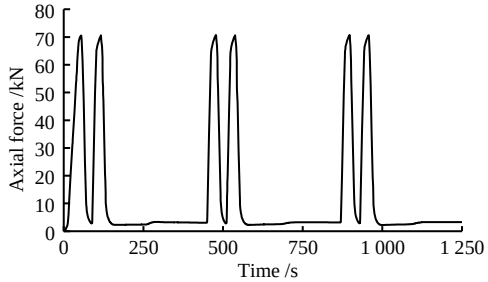

Fig. 10 Stress path of the interval fatigue test (5 min)

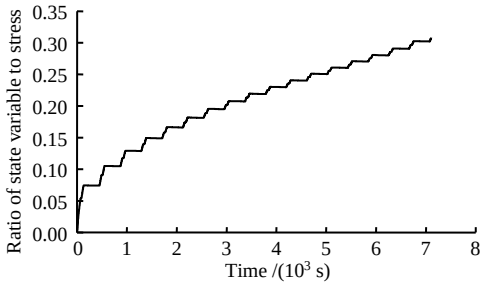

Fig. 11 Relation between state variable to stress ratio and time in the interval fatigue test (5 min)

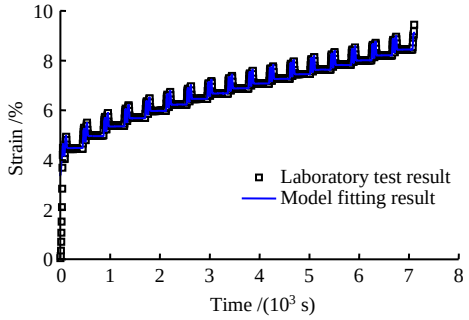

(a) Time interval is 5 min

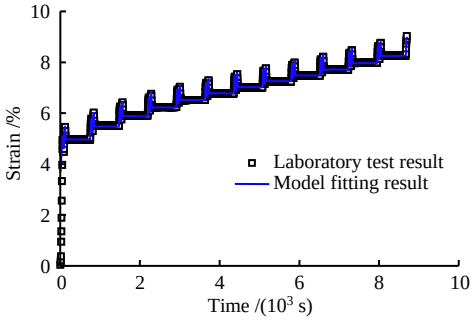

(b) Time interval is 10 min

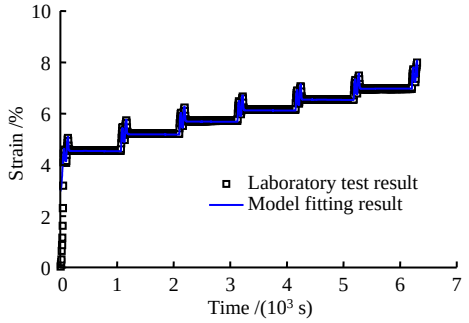

(c) Time interval is 15 min

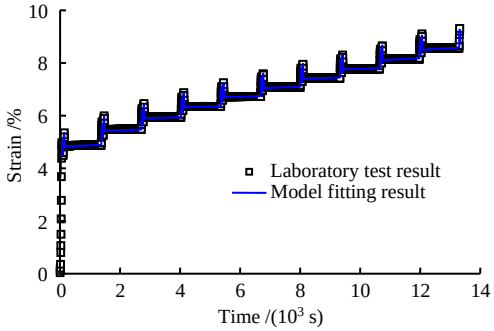

(d) Time interval is 20 min

Fig. 12 Comparisons between model fitting results and laboratory test data of the interval fatigue test

Table 4 Model parameters of the interval fatigue test

Time /min	*a*	*b*	*c*	*n*	*m*	*k*
5	36	15.6	345	1.1	1.10	–072
10	24	14.6	300	0.9	0.92	–0.72
15	25	15.0	280	0.9	0.92	–0.72
20	44	15.0	360	0.85	0.92	–0.72

From Figs. 11 and 12, it is observed that the change of state variable to stress ratio is consistent with the variation of strain, and both of them increase with time. In one cycle, there are two consecutive loading and unloading actions. In Fig. 11, it is found that when the salt rock is under constant loading, the state variable to stress ratio is constants, while the ratio increases continuously as the salt rock is under loading and unloading conditions, but there is an inflection point when unloading is performed within the first cycle. Based on the analysis of trapezoidal wave test, the state variable to stress ratio remains almost constant during unloading. Under the interaction of creep and fatigue, the results also indicate that the deformation recovery of salt rocks is damaged gradually during loading, while it is less affected during constant loading or unloading.

From the comparison between the model fitting results and the test data in Fig. 12, the proposed model can better predict the deformation process of salt rocks under the lower-limit interval cyclic loading and unloading. By selecting a cycle for comparison, it is found that the strain increases in the loading and unloading tests of two consecutive cycles, but the strain of salt rocks does not change significantly under static stress due to the small constant load (2 kN) and the short time, and the generated deformation of the specimen is almost negligible.

On the whole, for the lower-limit intervals with different stresses, the proposed model has a high consistency in the overall prediction results of cyclic loading and unloading. The variation of state variable to stress ratio can describe the interaction between creep and fatigue during the deformation process. From the model fitting results, one can see that the model can better fit the deformation of salt rocks under the interaction of creep and fatigue, indicating that the model has a good applicability.

4 Model analysis

Through the comparison of model fitting results and test data under the above four stress paths, it is found that the established creep–fatigue constitutive model can better predict the plastic deformation behavior of salt rocks under complex paths. In this section, several sets of key parameters in the model will be analyzed to determine the influence of relevant parameters on the model.

4.1 Influencing factor of deformation at the 2nd stage (influence of parameter *a*)

By merely changing the value of parameter a in the model, and keeping the stress and other parameters the same ($b=5$, $d_0=0.1$, $\mu_d=0.000\ 1$), different creep deformation curves can be obtained, as shown in Fig. 13. From Fig. 13(a), it can be seen that at the first two stages, the curves of variable-speed creep strain almost completely overlap, and the difference appears at the end of the 3rd stage. The change of parameter a has little effect on the variable-speed creep deformation of salt rocks. From the steady creep strain curve (Fig. 13(b)), one can see that the steady creep strain varies linearly, which means that the value of parameter a directly affects the slope of the straight line (i.e. the steady creep strain rate), and the larger the value of parameter a, the greater the rate of creep strain. From Fig. 13(c) of the total creep strain curve, it is found that the 3rd stage of deformation is mainly influenced by parameter a.

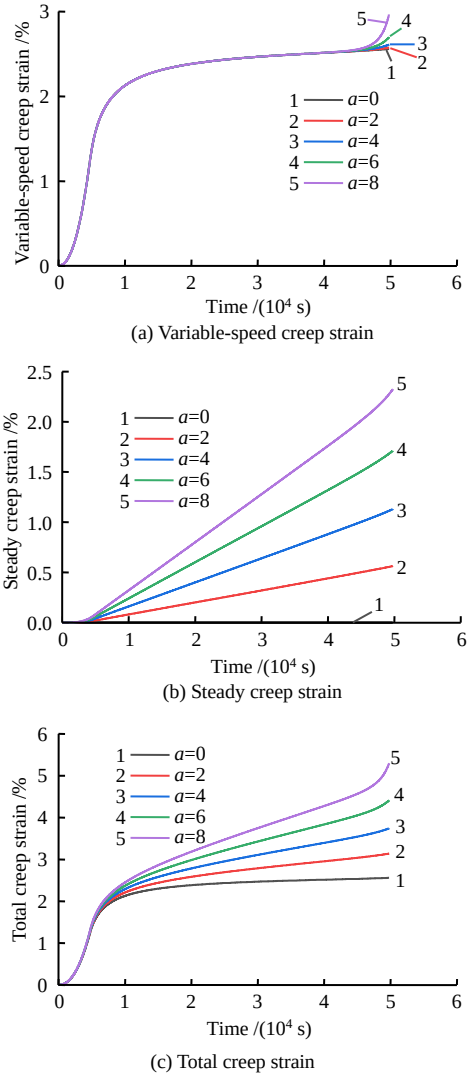

(a) Variable-speed creep strain

(b) Steady creep strain

(c) Total creep strain

Fig. 13 Creep strain curves with different values of parameter *a*

4.2 Influencing factor of deformation at the 1st stage (influence of parameter *b*)

When merely changing the value of parameter b in the model and keeping the stress and other parameters the same ($a=5$, $d_0=0.1$, $\mu_d=0.000\ 1$), different creep deformation curves can be obtained, as shown in

Fig. 14. From Fig. 14, it is observed that as the value of parameter *b* increases, the strain and the radius of curvature both increase during the variable-speed creep of salt rocks, as well as the corresponding strain at the same time (Fig. 14(a)). However, the change of parameter *b* has almost no effect on the steady creep. The strain curve at steady creep changes in a linear trend and the curves overlap with different *b* values (Fig. 14(b)). From the 1st stage to the 2nd stage, the radius of curvature of the final total creep strain curve (Fig. 14(c)) increases with the increasing of parameter *b*, and the strain curve at the 2nd stage is approximately a parallel straight line. Overall, the creep deformation of salt rocks at the 1st stage is mainly influenced by parameter *b*.

4.3 Influencing factors of deformation at the 3rd stage (influence of parameters d_0 and μ_d)

When merely changing the value of parameter d_0 (with $\mu_d = 0.000\ 1$) or μ_d (with $d_0 = 0.1$), with the same stress and other parameters ($a = 5$, $b = 5$), different creep deformation curves can be obtained, as shown in Fig. 15.

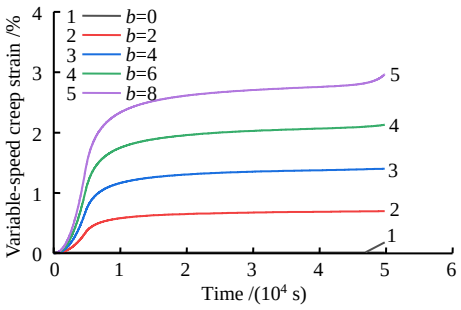

(a) Variable-speed creep strain

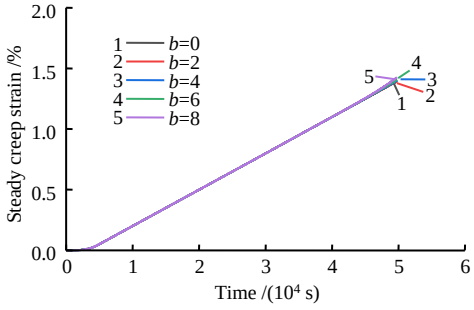

(b) Steady creep strain

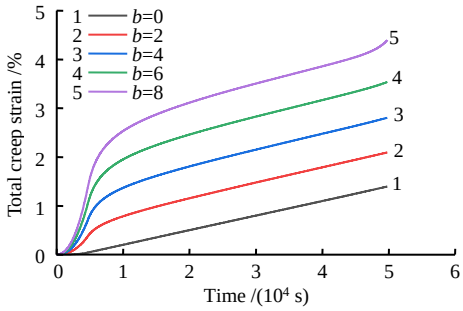

(c) Total creep strain

Fig. 14 Creep strain curves with different values of parameter *b*

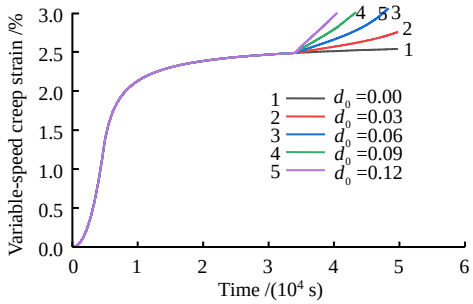

(a) Variable-speed creep strain with different d_0 values (μ_d =0.000 1)

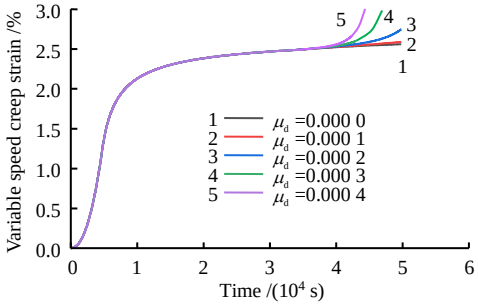

(b) Variable-speed creep strain with different μ_d values (d_0 =0.10)

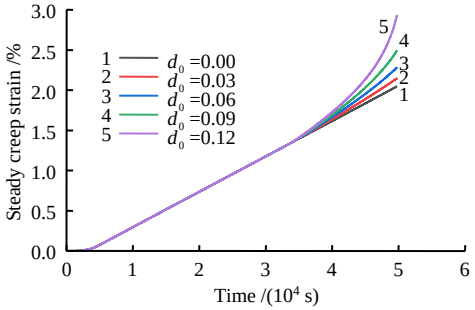

(c) Steady creep strain with different d_0 values (μ_d =0.000 1)

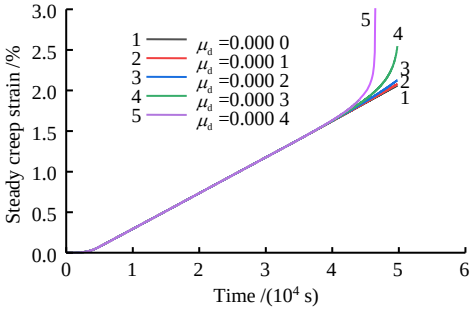

(d) Steady creep strain with different μ_d values (d_0 =0.10)

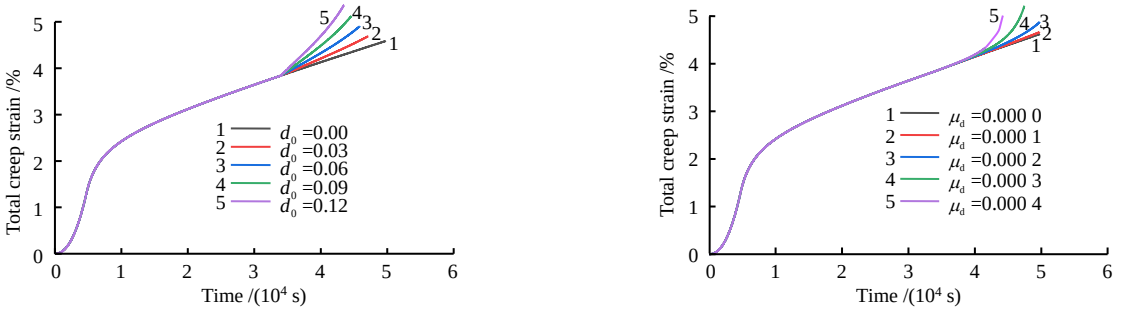

(e) Total creep strain with different d_0 values (μ_d =0.000 1)

(f) Total creep strain with different μ_d values (d_0 =0.10)

Fig. 15 Creep strain curves with different values of parameters d_0 and μ_d

From Fig. 15, it is shown that the changes of parameters d_0 ($\mu_d = 0.000\ 1$) and μ_d ($d_0 = 0.10$) have no effect on the 1st and 2nd stages of creep strain of salt rocks, and the curves coincide exactly. The 3rd stage of creep is affected by different d_0 and μ_d values, and the variable-speed creep strain and the steady creep strain of salt rocks increase with the increasing of d_0 or μ_d value. It should be pointed out that when the d_0 value increases, the corresponding variable-speed creep strain increases suddenly and linearly from one point, and the steady creep strain increases smoothly. While as μ_d value increases, variable-speed creep strain and steady creep strain are increasing in a circular curve, and the radius of curvature decreases as the μ_d value increases. In general, the 3rd stage of creep deformation for salt rocks is mainly influenced by the d_0 and μ_d values together.

5 Conclusions

By defining a hardening parameter and then introducing unloading factor and crack expansion factor, a new creep–fatigue constitutive model is established. Based on the unloading and loading test results of salt rocks under four stress paths, data analysis and model prediction are conducted to compare and analyze the model accuracy and the related parameter characteristics. The main conclusions are drawn as follows:

(1) The influences of different stress paths on the fatigue–creep of salt rocks are studied. By introducing the state variable to characterize the hardening degree of rock, a new creep–fatigue constitutive model of salt rocks is established considering loading and unloading history. Based on the proposed creep–fatigue constitutive model with hardening state variables, the deformation of salt rocks is divided into elastic deformation and creep deformation, and the creep strain is further divided into two parts: variable-speed creep strain and steady creep strain.

(2) Four loading paths are used to verify the fatigue–creep constitutive model, including constant load creep test, cyclic loading and unloading fatigue tests, trapezoidal wave creep–fatigue test, and lower-limit interval cyclic loading and unloading fatigue tests. The comparisons between the fitting and test curves of four stress paths show good agreements. When considering the effects of time, load and state on the creep–fatigue of salt rocks, it shows that the developed model can well describe the fatigue–creep plastic deformation characteristics of salt rocks under different stress paths.

(3) By analyzing the influences of different parameters on the model, the influences of different parameters on the creep of salt rocks are obtained. The parameter a mainly affects the 2nd stage of the creep–fatigue model, and the steady creep strain rate increases as the a value increases. The parameter b mainly affects the 1st stage of the creep–fatigue model. The variable-speed creep strain rate increases as the b value increases, and the radius of curvature also increases as b value increases from the 1st stage to the 2nd stage. The d_0 and μ_d values jointly affect the 3rd stage of creep–fatigue deformation of salt rocks.

References

[1] XI Bao-ping, ZHAO Yang-sheng. Investigation on stability of gas storage caverns in bedded rock salt[J]. Chinese Journal of Underground Space and Engineering, 2007, 3(Suppl.2): 1562–1567.

[2] ZHANG Fu-qiang, ZENG Ping, ZHOU Li-jian, et al. Underground gas storage research status quo and application expectations at home and abroad[J]. Coal Geology of China, 2021, 33(10): 39–42.

[3] LIU Wei, LI Yin-ping, YANG Chun-he, et al. Investigation on permeable characteristics and tightness evaluation of typical interlayers of energy storage caverns in bedded salt rock formations[J]. Chinese Journal of Rock Mechanics and Engineering, 2014, 33(3): 500–506.

[4] LI Peng, LI Yin-ping, SHI Xi-lin, et al. Evaluation of void characteristics and gas storage capacity of hydromining sediment in multi-layered salt mines[J]. Rock and Soil Mechanics, 2022, 43(1): 76–86.

[5] YANG Hua. Stability analysis of the underground gas storage in salt rock in the process of compressed air energy storage[D]. Wuhan: Graduate School of Chinese Academy of Sciences (Institute of Rock and Soil Mechanics), 2009.

[6] JIA Chao, ZHAN Qiang-yong, LIU Jia-tao, et al. Reliability analysis for underground salt rock gas storage under different gas pressures[J]. Chinese Journal of Underground Space and Engineering, 2011, 7(2): 276–280.

[7] YANG Chun-he, BAI Shi-wei, WU Yi-min. Stress level and loading path effect on time dependent properties of salt rock[J]. Chinese Journal of Rock Mechanics and Engineering, 2000, 19(3): 270–275.

[8] WANG J B, ZHANG Q, SONG Z P, et al. Creep properties and damage constitutive model of salt rock under uniaxial compression[J]. International Journal of Damage Mechanics, 2020, 29(6): 902–922.

[9] ZHANG X, LIU Wi, CHEN J, et al. Large-scale CO_2 disposal/storage in bedded rock salt caverns of China: an evaluation of safety and suitability[J]. Energy, 2022, 249. 123727.

[10] GAO R B, WU F, CHEN J, et al. Study on creep characteristics and constitutive model of typical argillaceous salt rock in energy storage caverns in China[J]. Journal of Energy Storage. 2022, 50: 104248.

[11] CHEN Jie, LIU Jian-wen, JIANG De-yi, et al. An experimental study of strain and damage recovery of salt rock under confining pressures[J]. Rock and Soil Mechanics, 2016, 37(1): 106–112.

[12] WU Chi, LIU Jian-feng, ZHOU Zhi-wei, et al. Study on creep properties of salt rock with impurities during triaxial creep test[J]. Advanced Engineering Sciences, 2017, 49(Suppl.2): 165–172.

[13] LIANG Wei-guo, XU Su-guo, ZHAO Yang-sheng. Investigation on solution pervasion and mechanical characteristics of glauberite salt rock[J]. Chinese Journal of Rock Mechanics and Engineering, 2006, 25(5): 951–955.

[14] LIU Di, ZHOU Hong-wei, ZHAO Yang, et al. Study of creep constitutive model of rock salt based on acoustic emission characteristics[J]. Rock and Soil Mechanics, 2017, 38(7): 1951–1958.

[15] XUE Bing, LIN Jia-wei, LIU Ji-cheng, et al. Direct shear tests on a Pakistan rock salt[J]. Soil Engineering and Foundation, 2021, 35(2): 234–237.

[16] HOU Zhi-qiang, WANG Yu, LIU Dong-qiao, et al. Experimental study on mechanical properties of marble under triaxial fatigue-unloading confining pressure[J] Rock and Soil Mechanics, 2020, 41(5): 1510–1520.

[17] ZHANG Qiang, WANG Jun-bao, SONG Zhan-ping, et al. Microstructure variation and empirical fatigue model of salt rock under cyclic loading[J]. Rock and Soil Mechanics, 2022, 43(4): 995–1008.

[18] WANG Yun-xiao, MA Lin-jian, DONG Lu, et al. Progress of research on rock creep-fatigue interaction properties[J]. Protective Engineering, 2020, 42(6): 31–41.

[19] ROBERTS L A, BUCHHOLZ S A, MELLEGARD K D, et al. Cyclic loading effects on the creep and dilation of salt rock[J]. Rock Mechanics and Rock Engineering, 2015, 48: 2581–2590.

[20] LI Zong-ze, JIANG De-yi, FAN Jin-yang, et al. Experimental study of triaxial interval fatigue of salt rock[J]. Rock and Soil Mechanics, 2020, 41(4): 1305–1312.

[21] ZHAO K, MA H L, ZHOU J, et al. Rock salt under cyclic loading with high-stress intervals[J]. Rock Mechanics and Rock Engineering, 2022, 55(7): 4031–4049.

[22] MA L J, WANG Y X, WANG M Y, et al. Mechanical properties of rock salt under combined creep and fatigue[J]. International Journal of Rock Mechanics and Mining Sciences, 2021, 141, 104654.

[23] LUO Ting, YAO Yang-ping. Method for developing hardening parameter independent of stress path for geomaterials[J]. Rock and Soil Mechanics, 2007, 28(1): 69–76.

[24] YANG Chun-he, MA Hong-ling, LIU Jian-feng. Study of deformation of rock salt under cycling loading and unloading[J]. Rock and Soil Mechanics, 2009, 30(12): 3562–3568.

[25] ZHOU Hong-wei, WANG Chun-ping, DUAN Zhi-qiang, et al. Time-based fractional derivative approach to creep constitutive model of salt rock[J]. Science China — Physics, Mechanics & Astronomy, 2012, 42(3): 310–318.

[26] ZHOU H W, WANG C P, HAN B B, et al. A creep constitutive model for salt rock based on fractional derivatives[J]. Rock Mechanics and Mining Sciences, 2011, 48(1): 116–121.

[27] PENG Fang-le, LI Fu-lin, BAI Xiao-yu, et al. Elasto-viscoplastic constitutive model of sandy soil considering stress path and loading rate[J]. Chinese Journal of Rock Mechanics and Engineering, 2009, 28(5): 929–938.

[28] YANG Chun-he, BAI Shi-wei, WU Yi-min. Stress level and loading path effect on time dependent properties of salt rock[J]. Chinese Journal of Rock Mechanics and Engineering, 2000, 19(3): 270–275.

[29] WU Fei, XIE He-ping, LIU Jian-feng, et al. Experimental study of fractional viscoelastic-plastic creep model[J]. Chinese Journal of Rock Mechanics and Engineering, 2014, 33(5): 964–970.

[30] LI Z Z, YANG F, FAN J Y, et al. Fatigue effects of discontinuous cyclic loading on the mechanical characteristics of sandstone[J]. Bulletin of Engineering Geology and the Environment, 2022, 81(8), 336.

[31] DING Jing-yang, ZHOU Hong-wei, CHEN Qiong, et al. Characters of rheological damage and constitutive model of salt rock[J]. Rock and Soil Mechanics, 2015, 36(3):

769–776.

[32] SHE Cheng-xue. Research on nonlinear viscoelasto-plastic creep model of rock[J]. Chinese Journal of Rock Mechanics and Engineering, 2009, 28(10): 2006–2011.

[33] ZHAO Yan-lin, CAO Ping, WEN You-dao, et al Elastovisco-plastic rheological experiment and nonlinear rheological model of rocks[J]. Chinese Journal of Rock Mechanics and Engineering, 2008, 27(3): 477–486.

[34] LIU Jian-feng, BIAN Yu, ZHENG De-wen, et al. Discussion on strength analysis of salt rock under triaxial compressive stress[J]. Rock and Soil Mechanics, 2014, 35(4): 919–925.

[35] CHEN Wei-zhong, WANG Zhe-chao, WU Guo-jun, et al. Nonlinear creep damage constitutive model of rock salt and its application to engineering[J]. Chinese Journal of Rock Mechanics and Engineering, 2007, 26(3): 467–472.

[36] PENG Rui-dong, WU Zhi-de, ZHOU Hong-wei, et al. Meso-experimental investigation on crack evolution in bedded salt rock[J]. Chinese Journal of Rock Mechanics and Engineering, 2011, 30(Suppl.2): 3953–3959.

[37] ZHANG Yu-zhuo, ZHONG Wei-lin, YAO Jian-guo. Theoretical solution of dislocation and boundary element method for studying strata movements[J]. Journal of China Coal Society, 1987(2): 21–31.